

闪电等离子体连续光谱轮廓形成机理研究

董向成 王国伟 陈建宏

Formation mechanism of the continuous spectral profile of lightning plasma

DONG Xiang-cheng, WANG Guo-wei, CHEN Jian-hong

引用本文:

董向成, 王国伟, 陈建宏. 闪电等离子体连续光谱轮廓形成机理研究[J]. 中国光学, 2021, 14(5): 1243-1250. doi: 10.37188/CO.2021-0018

DONG Xiang-cheng, WANG Guo-wei, CHEN Jian-hong. Formation mechanism of the continuous spectral profile of lightning plasma[J]. *Chinese Optics*, 2021, 14(5): 1243-1250. doi: 10.37188/CO.2021-0018

在线阅读 View online: <https://doi.org/10.37188/CO.2021-0018>

您可能感兴趣的其他文章

Articles you may be interested in

人工触发闪电通道的辐射特性分析

Analysis of radiation evolution characteristics of the artificial triggered lightning channel

中国光学. 2019, 12(3): 670 <https://doi.org/10.3788/CO.20191203.0670>

表面等离子体平面金属透镜及其应用

Planar plasmonic lenses and their applications

中国光学. 2017, 10(2): 149 <https://doi.org/10.3788/CO.20171002.0149>

基于光电探测的多光谱测温装置

Multi-spectral temperature measuring system based on photoelectric detection

中国光学. 2019, 12(2): 289 <https://doi.org/10.3788/CO.20191202.0289>

酞菁化合物合成及光谱性能研究

Synthesis and spectral properties of phthalocyanine compounds

中国光学. 2018, 11(5): 765 <https://doi.org/10.3788/CO.20181105.0765>

树基沟矿区铜胁迫落叶松的光谱响应特征研究

Spectral reflected response of Larch to copper stress in Shujigou mining area

中国光学. 2019, 12(2): 332 <https://doi.org/10.3788/CO.20191202.0332>

紫铜粗糙表面的光谱双向反射分布函数测量研究

A study on the spectral BRDF measurement of red copper rough surfaces

中国光学. 2019, 12(6): 1385 <https://doi.org/10.3788/CO.20191206.1385>

Formation mechanism of the continuous spectral profile of lightning plasma

DONG Xiang-cheng^{1*}, WANG Guo-wei¹, CHEN Jian-hong²

(1. BaiLie School of Petroleum Engineering, Lanzhou City University, Lanzhou 730070, China;

2. School of Electronic and Information Engineering, Lanzhou City University, Lanzhou 730070, China)

* Corresponding author, E-mail: dongxiangc@tom.com

Abstract: The cloud-to-ground lightning discharge spectrum was recorded using a slitless grating spectrograph with a spectral range of 400~1 000 nm. Abundant monovalent nitrogen ion lines were observed in the lower-frequency range of the visible spectra, whereas other important ion lines were not clearly observed. Under the action of the cloud-to-ground electric field, a large number of electrons in the lightning plasma channel poured onto the ground and quickly heated the channel, such that the temperature decreased along the radial direction of the channel. This process enhanced the interaction between the nitrogen ions and the electrons near the channel surface, producing continuous radiation. The continuous radiation mechanism of lightning mainly includes bremsstrahlung and recombination radiation, which correspond to the Coulomb collision between the nitrogen ions and free electrons and the capture of free electrons. When the plasma temperature is lower than 10,000 K, the continuous bremsstrahlung spectrum is a flat spectrum, which has no obvious influence on the profile characteristics of the continuous spectrum in the visible light range. For recombination radiation, an approximate calculation method for non-hydrogen-like complex ions was introduced on the basis of the classic hydrogen-like ion radiation theory. The Gaunt factor was used for quantum mechanic correction to analyze the recombination radiation process of nitrogen ions, on the basis of above, the functional relationship between the recombination radiation coefficient of the continuous spectrum and the wavelength was derived. Finally, a characteristic curve was drawn for the continuous radiation spectrum of nitrogen plasma. The curve was compared with the observed profile of the continuous lightning spectrum, revealing that the temperature of the electrons on the plasma surface is closely related to the position of the continuous radiation spectrum peak; the effective nuclear charge number Z^* of the introduced nitrogen ions has a significant effect on step feature and broadening characteristics of the continuum spectrum. By comparison, when Z^* was set to 3, the theoretical curve was highly consistent with the profile characteristics of the continuous spectrum. The range of Z^* was determined by the type of ions. The introduction of Z^* could help to effectively explain the step feature of the continuous spectrum of the lightning plasma at a given wavelength.

Key words: lightning spectra; continuous radiation; spectral profile feature; electron temperature

收稿日期:2021-01-27; 修订日期:2021-03-18

基金项目:国家自然科学基金资助项目(No. 12064023); 兰州市科技发展指导性计划资助项目(No. 2019-ZD-172)

Supported by the National Natural Science Foundation of China (No. 12064023); Lanzhou Science and Technology Development Guidance Plan Project (No. 2019-ZD-172)

闪电等离子体连续光谱轮廓形成机理研究

董向成^{1*}, 王国伟¹, 陈建宏²

(1. 兰州城市学院 培黎石油工程学院, 甘肃兰州, 730070;

2. 兰州城市学院 电子与信息工程学院, 甘肃兰州, 730070)

摘要:利用光谱范围为 400~1000 nm 的无狭缝光栅光谱仪记录了云对地闪电放电光谱, 在可见光谱的低频段观测到丰富的一价氮离子谱线, 没有明显观测到其他重要的离子谱线。闪电通道内大量电子在电场作用下向地面倾泻使通道快速加热, 沿通道径向温度降低, 通道表面附近氮离子与电子的相互作用增强从而产生连续辐射。闪电的连续辐射机制主要包括韧致辐射和复合辐射, 对应于氮离子与自由电子的库仑碰撞和对自由电子的捕获。当等离子体温度低于 10000 K 时, 韧致连续辐射谱为平坦谱, 其对连续谱在可见光范围内的轮廓特征没有明显影响。复合辐射方面, 以类氢离子经典辐射理论为基础, 引入非类氢的复杂离子近似计算方法, 用 Gaunt 因子进行量子力学修正, 分析氮离子的复合辐射过程。据此导出连续光谱复合辐射系数与波长的函数关系, 由关系式绘制氮等离子体连续辐射光谱的特征曲线, 与闪电连续光谱观测结果进行比较, 发现等离子体表面电子温度与连续辐射光谱谱峰的位置密切相关; 引入氮离子的有效核电荷数 Z 对连续谱的阶跃特征和谱翼展宽特性有显著影响。对比发现, 当 Z 为 3 时, 理论曲线与连续光谱的轮廓特征高度一致。 Z 的取值范围由离子种类决定, 有效核电荷数 Z 能很好地解释闪电等离子体在给定波长下连续光谱的阶跃特征。

关键词: 闪电光谱; 连续辐射; 谱轮廓特征; 电子温度

中图分类号: O433

文献标志码: A

doi: 10.37188/CO.2021-0018

1 Introduction

Plasma spectroscopy is a focus of frontier research and has broad application prospects in fields such as space physics, high-voltage breakdown and material processing^[1]. Lightning is a type of common natural atmospheric gas discharge plasma. There are many types of particles in lightning discharge plasma, that collide with one other frequently, accompanied by an increasingly violent discharge process^[2], hampering direct measurement of its parameters, thus making spectrometry an important means of indirectly measuring and studying its characteristics. Lightning plasma spectra are characterized by superposition of line spectra over strongly continuous spectra, which are closely related to the initiation, stabilization and disappearance of the lightning, thereby significantly impacting the accurate measurement of the linear spectra^[3]. Many results have been achieved in research on the linear spectra of lightning. Owing to the complexity of the formation mechanism of continuous spectra,

there remain few studies on the continuous radiation spectra of plasma. So, it is of great significance to research the development and dissipation of low-temperature thermal plasma and the process of energy transmission inside plasma.

In the process of cloud-to-ground discharge, lower atmospheric changes have a higher research value. The lower atmospheric layer consists of clean dry air, water vapor, and pollutants, of which clean dry air is the main component. To simplify the analysis process, atmospheric ionization by lightning is reducible to the ionization of clean dry air. Nitrogen is the major component of clean dry air, accounting for about 78.08% by volume, while oxygen accounts for about 20.95% and inert gases account for about 0.93%. The generation of lightning plasma is mainly due to nitrogen and oxygen. When the equilibrium temperature of the gases is about 10,000 K, all oxygen and nitrogen molecules are in the atomic state^[4-5], and the typical temperature of the lightning discharge return stroke channel is normally 10,000 K. So, without considering the molecular spectra in the channel^[6], after elimination of stray light, the con-

tinuous spectra are determined by the bremsstrahlung and recombination radiation processes.

2 Theoretical methodology

2.1 Effect of bremsstrahlung on continuous spectra

Bremsstrahlung is generated by a sudden change in the speed of electron motion in plasma. It is divided into electronic-atomic bremsstrahlung generated by electrons under the action of the nuclear electric field, and electronic-ionic bremsstrahlung generated under the action of the ion Coulomb field. The avalanche of ionization energy generated in the formation process of a lightning channel highly ionizes the center of the channel. Considering the very low atomic density inside, the effect of electronic-atomic bremsstrahlung on the continuous spectra can be ignored. The high temperature in the return stroke channel drives ions toward the thermal equilibrium state, and the electron velocity follows the Maxwell distribution. Electrons at various initial velocities contribute to the monochromatic radiation waves within the range. The radiation coefficient for the collective spectra of the thermal equilibrium plasma electrons with temperature T_{in} is^[7-11]:

$$J_{ff}(T_{in}, \lambda) = C_1 \frac{1}{\lambda^2} \frac{1}{\sqrt{T_{in}}} \exp\left(-\frac{hc}{\lambda k T_{in}}\right), \quad (1)$$

where $C_1 = 5.44 \times 10^{-52} \cdot c \cdot Z^2 \cdot N_e \cdot N_Z \cdot g_{ff}(T_{in}, \lambda)$, in which N_e and N_Z respectively represent electron density and ion density; Z represents the ionic charge number; and $g_{ff}(T_{in}, \lambda)$ represents the mean Gaunt quantum mechanics revision factor. C_1 has no impact on the continuous spectral profile of bremsstrahlung, while the spectral intensity tends to rise first and then decrease as C_1 increases. The main factors affecting C_1 include electron density N_e and ion density N_Z . In a low-temperature plasma, owing to the low mean velocity of electrons, the $g_{ff}(T_{in}, \lambda)$ and the ionic charge number Z have little impact on C_1 . As can be seen from Equation (1), when the wavelength is less than 200 nm, the effect

of bremsstrahlung is significant. When the wavelength is greater than 200 nm, the bremsstrahlung is characterized by flat spectra. The experimental observation shows that the continuous spectral peak of lightning mainly appears between 400 nm and 600 nm, and bremsstrahlung has no appreciable impact on its profile features.

2.2 Effect of recombination radiation on continuous spectra

Freely moving electrons in plasma are captured by ions, producing recombination radiation as they bind. The higher the plasma temperature, the greater the average kinetic energy of the electrons, and the higher the frequency of the continuous radiation. After being captured by ions, the electrons may be in a highly excited state, and the atomic spectra generated during electron transition to a lower level is known as complex-cascade radiation recombination radiation. It contributes to the monochromatic radiation waves within the range. For local thermal equilibrium hydrogen plasma with a temperature of T_{ex} , the recombination radiation coefficient in the channel is represented by^[7-11]:

$$J_{fb}(T_{ex}, \lambda) = 5.44 \times 10^{-52} \frac{c \cdot Z^4 \cdot N_e \cdot N_Z}{\lambda^2} \cdot \left(\frac{1}{T_{ex}}\right)^{\frac{3}{2}} \cdot \exp\left(1 - \frac{hc}{\lambda k T_{ex}}\right) \frac{g_{i,1}}{U_i} g_{fb}(T_{ex}, \lambda), \quad (2)$$

where $g_{i,1}$ represents the statistical weight of ground-state ions, and U_i is a partition function. For a hydrogen plasma in excited state, $g_{i,1} \approx U_i$, and $g_{fb}(T_{ex}, \lambda)$ represents the average Gaunt factor of the recombination radiation.

The above theory is applicable to hydrogen and hydrogen-like plasmas. For lightning plasma, it can be improved through parameter correction and approximation based on an analysis of the spectral features of lightning. A slitless spectrograph consisting of a high-speed camera and a plane transmission grating with 600 lines/mm, was used to record a spectral image of a lightning return stroke in Qinghai, as shown in Figure 1. The high-speed camera was operated at 6000 frames per second (fps), and

the time interval between the two images in Figure 1 is 0.117 ms.

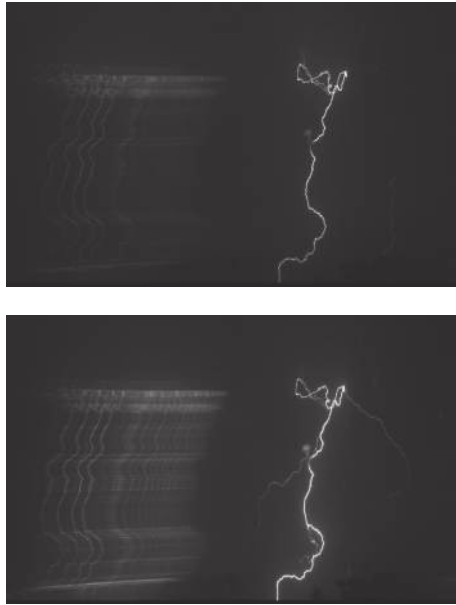


Fig. 1 Images of time-sharing lightning beam

The image was interpreted with reference to the National Institute of Standards and Technology (NIST) Atomic Spectra Database, obtaining spectra of the same beam at different heights from the ground, as shown in Figure 2. Figure 2(a) shows the spectrum at a high elevation while Figure 2(b) shows the spectrum at a low elevation. Figure 2 shows that the main component of the positive ions in the lightning plasma is N II, so equation (2) can not be completely suitable for analyzing the continuous spectra of lightning plasma and must be revised. Lightning spectra are quite similar to the spectra of welding arc plasma^[12]. The temperature is highest at the center of the discharge channel^[13] and the core current channel is very thin while the charge density is high. Thus, an electric field is generated radially from the channel, driving charges outward to form an electric light beam layer, with a gradually decreasing temperature. Therefore, the lightning channel is regarded as a plasma column whose temperature decreases from the inside out. The core current channel is at a high temperature and its continuous radiation is dominated by bremsstrahlung. The light beam layer outside the

channel is at a low temperature, and the continuous radiation is dominated by recombination radiation.

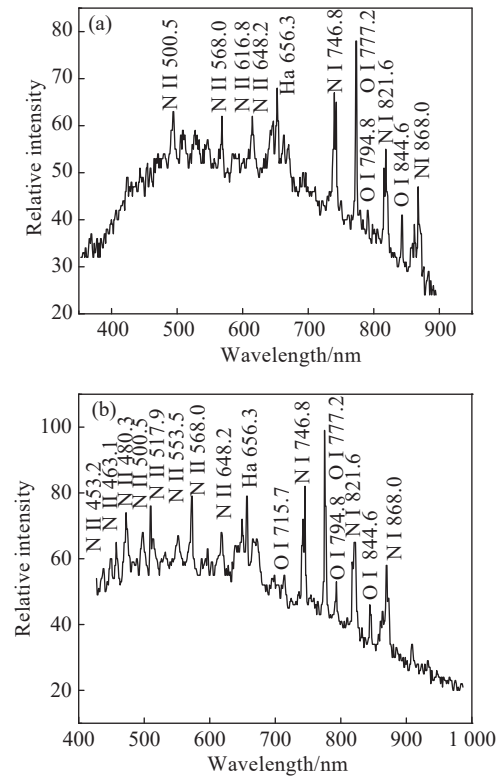


Fig. 2 Spectra of the lightning beam at different heights from the ground

Figure 2 shows a large number of N II spectral lines on the short-wave band, while other spectra are not clearly visible. Considering that continuous spectra are mainly generated by monovalent nitrogen ions, Equation (2) needs to be revised. Because electrons are very likely to enter a highly excited state when captured by ions, in approximation, nitrogen ions and electrons form a hydrogen-like system. The energy of the electrons for photon radiation in the complex process is as follows:

$$h\nu = \frac{1}{2}m_e V_e^2 + (E_1 - E_n) \quad , \quad (3)$$

where E_1 represents the first ionization energy 14.53 eV of the nitrogen atoms; E_n represents the n^{th} excitation energy of the nitrogen atoms, $E_\infty = 0$ is its minimum, while the first ionization energy of nitrogen atoms is its maximum. Formula (3) shows that continuous radiation spectra are not smooth in the recombination radiation process. A transition

peak exists at E_n and the ionization energy $E_1 - E_n \leq hv$, compounded to all n energy levels, affects the total emission coefficient of the continuous radiation. The ionization energy ($E_1 - E_n$) at the n^{th} energy level can be approximately represented as the ionization energy of hydrogen atoms.

$$hv \geq E_1 - E_n \approx \frac{(Z^*)^2 R_y}{n^2}, \quad (4)$$

where R_y represents the Rydberg energy, and Z^* represents the effective charge number in nitrogen ions. Thus, the value of $n(\lambda)$ can be determined as follows:

$$n(\lambda) = Z^* \sqrt{\frac{R_y \lambda}{hc}}. \quad (5)$$

The value of Z^* should be between 2 and 7, so Equation (2) is revised as follows:

$$J_{\text{fb}}(T_{\text{ex}}, \lambda) = \frac{C_2}{\lambda^2} \cdot \left(\frac{1}{T_{\text{ex}}}\right)^{\frac{3}{2}} \exp\left(\frac{E_{1,n}}{kT_{\text{ex}}} - \frac{hc}{\lambda kT_{\text{ex}}}\right) \times \sum G_n(\lambda) \cdot n^{-3} \cdot \exp\left(-\frac{E_n}{kT_{\text{ex}}}\right), \quad (6)$$

where $C_2 = 5.44 \times 10^{-52} \cdot c \cdot Z^4 \cdot N_e \cdot N_Z$, in which C_2 has no impact on the continuous shape of the recombination radiation spectra, and $E_{1,n}$ represents the energy released by the electrons when captured at the n^{th} energy level. Low-temperature thermal plasma $G_n(\lambda)$ can be set as a function that decreases linearly from 5 to 1 as the wavelength increases^[14-15].

3 Comparison between the profile features of the theoretical and experimental continuous spectra curves

3.1 Characteristics of the theoretical curve

The wavelength is set to 200–1200 nm. The surface temperature of the plasma column T_{ex} is set to $8 \times 10^3 - 1.2 \times 10^4 \text{K}$, $E_{1,n} = 1 \text{eV}$, $E_n = 13.6 \text{eV}$, and Z^* is set to 2–5.

Lightning plasma is considered to be optically thin, so the spectral intensity is positively correlated with the radiation coefficient of the spectra^[16, 17]. The

functional curve of the spectral radiation coefficient is compared with the profile of the continuous radiation spectrum. As shown in Figure 3(a), as Z^* increases, the transition features of the spectral shape weaken, as does the radiation intensity. This can be interpreted as a decrease in the probability that free electrons are captured into the inner orbit of the ions. As shown in Figure 3(b), as the plasma temperature T_{ex} increases, the continuous spectral peak shifts significantly toward the short-wave, and the radiation intensity changes slightly. This can be interpreted as a violet shift of the continuous spectra caused by an increase in the proportion of high-energy free electrons.

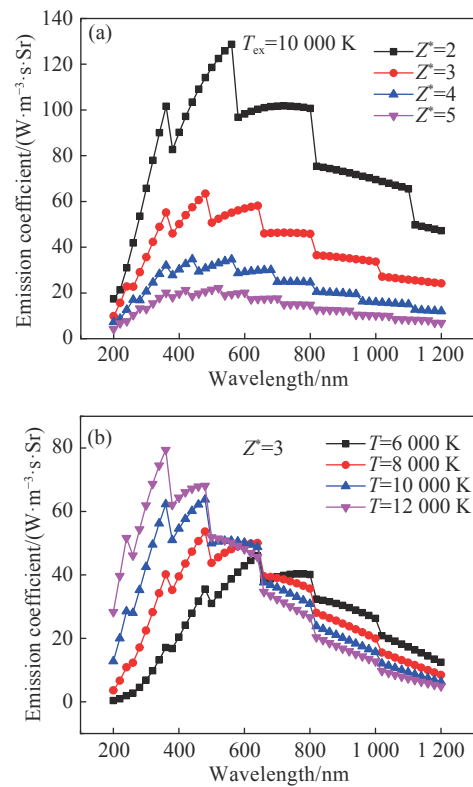


Fig. 3 Effect of T_{ex} and Z^* on the profile features of the continuous spectra

The continuous spectral envelope in Figure 2 is extracted and compared with the curve in Figure 3. Setting the temperature to 7,500 K and the effective charge number in the ions to 3, a continuous theoretical spectral profile is drawn and compared with the continuous spectral profile in Figure 2, as shown in Figure 4.

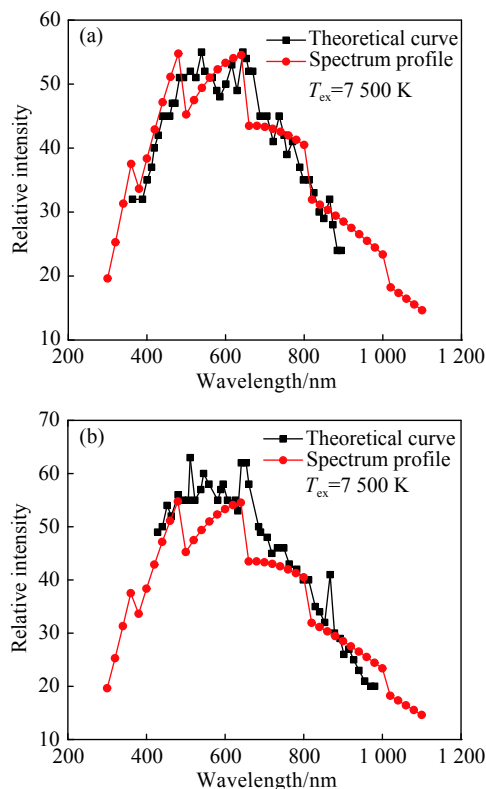


Fig. 4 Comparison between the experimental and theoretical profile features of the continuous spectra ($Z^*=3$)

As shown in Figure 4, the theoretical curve fits well with the experimental spectral profile. In Figure 4(b), the experimental spectral intensity is greater than the theoretical spectral intensity. This is because Figure 4(b) corresponds to the continuous spectra of the near-ground lightning plasma column. The ion density in the return stroke channel should be greater than the particle density corresponding to Figure 4(a). The calculation results show that the near-ground ion density in the return stroke channel is about 1.14 times that at the top.

3.2 Comparative feature analysis of the theoretical curve and experimental spectral profile

The comparison between the linear theoretical curve of continuous radiation spectra and the continuous spectral profile features of lightning spectra shows that bremsstrahlung contributes little to changes in the continuous spectral profile within the spectral frequency and temperature range of lightning plasma. It only affects the short-wave band with no significant effect on the medium or long-

wave bands^[18]. Quantum mechanics revision, a continuous radiation theory based on classical physics, was realized through the Gaunt factor, which is normally set to a constant close to or greater than 1 in low-temperature plasma. In contrast to welding arc plasma, the factor was set to a quantity that changed linearly with the wavelength. Taking the Gaunt factor into consideration, limb broadening was diminished on the theoretical continuous spectrum profile, becoming more consistent with the experimental profile. The plasma electron temperature showed the most significant effect on the profile. As the temperature rose, the spectral peak shifted toward the short-wave. As shown in Figure 4, the experimental spectral profile is most consistent with the theoretical curve at 7500 K. This result falls within the range of results defined by the continuous spectral slope method in Ref. [19]. Ion species is another important factor affecting the continuous spectral profile. The larger the atomic number of the ions, the weaker the transition features of the resulting continuum spectra.

4 Conclusions

The Gaunt factor has been used for quantum mechanics revision on the basis of the classical theory of hydrogen-like ions. Considering that free electrons are very likely to enter a highly excited atomic state, ions' effective charge number or ground-state ionization energy can be revised to approximate monovalent nitrogen ions by viewing them as hydrogen-like ions. This establishes a theoretical formula for the continuous spectral radiation coefficient of nitrogen plasma. The consistency between the continuous spectral profile features of the theoretical curve and lightning plasma was verified, revealing that plasma temperature has the most significant effect on the continuous spectral profile features and plays a major role in locating the spectral peak with respect to the wavelength. Second, the effective nuclear charge number following the approx-

imation of nitrogen ions as hydrogen-like ions plays a major role in promoting the appearance of the continuous spectral transition peak and also has an effect on the limb broadening of the continuous spectra.

References:

- [1] 苏风梅, 张达, 梁风. 低温等离子体制备与改性纳米催化材料的研究进展[J]. *应用化学*, 2019, 36(8): 882-891.
SU F M, ZHANG D, LIANG F. Progress in preparation and modification of nano-catalytic materials by low-temperature plasma[J]. *Chinese Journal of Applied Chemistry*, 2019, 36(8): 882-891. (in Chinese)
- [2] 李和平, 于达仁, 孙文廷, 等. 大气压放电等离子体研究进展综述[J]. *高电压技术*, 2016, 42(12): 3697-3727.
LI H P, YU D R, SUN W T, et al.. State-of-the-art of atmospheric discharge plasmas[J]. *High Voltage Engineering*, 2016, 42(12): 3697-3727. (in Chinese)
- [3] 张华明, 张义军, 吕伟涛, 等. 一次空中触发闪电通道光谱分析[J]. *光谱学与光谱分析*, 2018, 38(12): 3673-3677.
ZHANG H M, ZHANG Y J, LV W T, et al.. The spectra characteristic of altitude triggered lightning channel[J]. *Spectroscopy and Spectral Analysis*, 2018, 38(12): 3673-3677. (in Chinese)
- [4] 陈浩, 李林颖, 张斌, 等. Q-K模型在氮氧离解复合反应中的评估[J]. *空气动力学学报*, 2018, 36(1): 17-21.
CHEN H, LI L Y, ZHANG B, et al.. Assessment of Q-K model for nitrogen and oxygen dissociation-recombination[J]. *Acta Aerodynamica Sinica*, 2018, 36(1): 17-21. (in Chinese)
- [5] 李琳, 任慧敏, 卫博慧, 等. 钒-氮共掺杂碳基介孔纳米材料的制备及氮还原电催化性能[J]. *应用化学*, 2020, 37(8): 930-938.
LI L, REN H M, WEI B H, et al.. V-N Co-doped mesoporous carbon nanomaterials as catalysts for artificial N₂ reduction[J]. *Chinese Journal of Applied Chemistry*, 2020, 37(8): 930-938. (in Chinese)
- [6] 付宝勤, 侯氢, 汪俊, 等. 钨空位捕获氢及其解离过程的分子动力学[J]. *物理学报*, 2019, 68(24): 240201.
FU B Q, HOU Q, WANG J, et al.. Molecular dynamics study of trapping and detrapping process of hydrogen in tungsten vacancy[J]. *Acta Physica Sinica*, 2019, 68(24): 240201. (in Chinese)
- [7] CRESSAULT Y, GLEIZES A. Thermal plasma properties for Ar-Al, Ar-Fe and Ar-Cu mixtures used in welding plasmas processes: I. Net emission coefficients at atmospheric pressure[J]. *Journal of Physics D: Applied Physics*, 2013, 46(41): 415206.
- [8] IORDANOVA E, DE VRIES N, GUILLEMIER M, et al.. Absolute measurements of the continuum radiation to determine the electron density in a microwave-induced argon plasma[J]. *Journal of Physics D: Applied Physics*, 2008, 41(1): 015208.
- [9] PARK S, CHOE W, YOUN MOON S, et al.. Electron density and temperature measurement by continuum radiation emitted from weakly ionized atmospheric pressure plasmas[J]. *Applied Physics Letters*, 2014, 104(8): 084103.
- [10] KUNZE H J. *Introduction to Plasma Spectroscopy*[M]. Heidelberg Berlin: Springer, 2009.
- [11] VAN HOOFF P A M, FERLAND G J, WILLIAMS R J R, et al.. Accurate determination of the free-free Gaunt factor- II. Relativistic Gaunt factors[J]. *Monthly Notices of the Royal Astronomical Society*, 2015, 449(2): 2112-2118.
- [12] 张志芬, 杨哲, 任文静, 等. 电弧光谱深度挖掘下的铝合金焊接过程状态检测[J]. *焊接学报*, 2019, 40(1): 19-25.
ZHANG ZH F, YANG ZH, REN W J, et al.. Condition detection in Al alloy welding process based on deep mining of arc spectrum[J]. *Transactions of the China Welding Institution*, 2019, 40(1): 19-25. (in Chinese)
- [13] 张虎, 何建萍, 林杨胜蓝. 微束等离子弧焊电弧三维光谱及其抗干扰解耦[J]. *光谱学与光谱分析*, 2020, 40(1): 48-53.
ZHANG H, HE J P, LINYANG SH L. Three-dimensional arc spectrum and anti-interference decoupling in micro plasma arc welding[J]. *Spectroscopy and Spectral Analysis*, 2020, 40(1): 48-53. (in Chinese)
- [14] 刘玉峰, 丁艳军, 彭志敏, 等. 激光诱导击穿空气等离子体时间分辨特性的光谱研究[J]. *物理学报*, 2014, 63(20): 205205.
LIU Y F, DING Y J, PENG ZH M, et al.. Spectroscopic study on the time evolution behaviors of the laser-induced breakdown air plasma[J]. *Acta Physica Sinica*, 2014, 63(20): 205205. (in Chinese)
- [15] ZHANG M, YUAN P, LIU G R, et al.. The current variation along the discharge channel in cloud-to-ground lightning[J]. *Atmospheric Research*, 2019, 225: 121-130.

- [16] 王飞, 李桓, 杨珂, 等. 钨极稀有气体电弧辐射及其在能量平衡中的作用[J]. *光学学报*, 2018, 38(7): 0726001.
WANG F, LI H, YANG K, *et al.*. Tungsten inert gas welding arc radiation and its role in energy balance[J]. *Acta Optica Sinica*, 2018, 38(7): 0726001. (in Chinese)
- [17] 张华明, 吕伟涛, 张阳, 等. 人工触发闪电通道的辐射特性分析[J]. *中国光学*, 2019, 12(3): 670-676.
ZHANG H M, LV W T, ZHANG Y, *et al.*. Analysis of radiation evolution characteristics of the artificial triggered lightning channel[J]. *Chinese Optics*, 2019, 12(3): 670-676. (in Chinese)
- [18] DONG X CH, CHEN J H, WEI X F, *et al.*. Calculating the electron temperature in the lightning channel by continuous spectrum[J]. *Plasma Science and Technology*, 2017, 19(12): 125304.
- [19] 董向成, 袁萍. 连续辐射谱法计算闪电通道电子温度[J]. *光谱学与光谱分析*, 2018, 38(4): 1209-1212.
DONG X CH, YUAN P. Calculating the electron temperature of lightning channel based on the continuous radiation[J]. *Spectroscopy and Spectral Analysis*, 2018, 38(4): 1209-1212. (in Chinese)

Author Biographies:



DONG Xiang-cheng (1975 —), male, born in Baiyin City, Gansu province, Associate professor, BaiLie School of Petroleum Engineering, Lanzhou City University. His research interests are on the low temperature plasma and lightning physics. E-mail: dongxiangc@tom.com



CHEN Jian-hong (1982 —), male, born in Pingliang City, Gansu province, Doctor, Professor, School of Electronic and Information Engineering, Lanzhou City University. His research interests are on the plasma physics, and the atomic and molecular physics. E-mail: chenyuwen1982@163.com

《光学 精密工程》(月刊)

- 中国光学开拓者之一王大珩院士亲自创办的新中国历史最悠久的光学期刊
- 现任主编为国家级有突出贡献的青年科学家曹健林博士
- Benjamin J Eggleton, John Love 等国际著名光学专家为本刊国际编委

《光学 精密工程》主要栏目有现代应用光学(空间光学、纤维光学、信息光学、薄膜光学、光电技术及器件、光学工艺及设备、光电跟踪与测量、激光技术及设备);微纳技术与精密机械(纳米光学、精密机械);信息科学(图像处理、计算机应用与软件工程)等。

- * 美国工程索引 EI 核心期刊
- * 中国出版政府奖期刊提名奖
- * 中国精品科技期刊
- * 中文核心期刊
- * 百种中国杰出学术期刊
- * 中国最具国际影响力学术期刊

主管单位:中国科学院

主办单位:中国科学院长春光学精密机械与物理研究所
中国仪器仪表学会

地址:长春市东南湖大路 3888 号

邮编:130033

电话:0431-86176855

传真:0431-84613409

电邮:gxjmgc@sina.com

网址:http://www.eope.net

定价:100.00 元/册